Identification of Selected Gamma-Ray Induced Deficiencies in Zebrafish Using Multiplex Polymerase Chain Reaction

Andreas Fritz, Marion Rozowski, Charline Walker and Monte Westerfield

Institute of Neuroscience, University of Oregon, Eugene, Oregon 97403

Manuscript received June 11, 1996
Accepted for publication September 16, 1996

ABSTRACT

The ease with which mutations can be generated in zebrafish makes this vertebrate an important resource for developmental genetics and genome studies. We have developed a PCR-based screening method that allows the efficient identification of gamma-ray induced deficiencies targeted to selected sequences. We describe three mutants characteristic of our findings and show that these mutations include deletions and translocations that can affect as much as 1% of the genome. These deficiencies provide a basis for analyzing the functions of cloned zebrafish genes using noncomplementation screens for point mutations induced by high-efficiency chemical mutagenesis.

We describe here a reverse genetic approach to identify gamma-ray induced mutations affecting any cloned and sequenced zebrafish gene. A genetic approach has been successfully applied to elucidate developmental processes in the invertebrate organisms *Drosophila melanogaster* and *Caenorhabditis elegans*. Recently, large scale screens to identify and analyze mutations that disrupt developmental events have been carried out using the zebrafish (*Danio rerio*) (KIMMEL 1989; MULLINS and NÜSSLEIN-VOLHARD 1993; DRIEVER *et al.* 1994; MULLINS *et al.* 1994; NÜSSLEIN-VOLHARD 1994; SOLNICA-KREZEL *et al.* 1994; RILEY and GRUNWALD 1995). These screens employ a classical genetic strategy to isolate mutant phenotypes first before determining the identity of the affected genes. Despite significant progress in establishing a genetic map of the zebrafish genome (JOHNSON *et al.* 1996; POSTLETHWAIT *et al.* 1994), identifying the molecular nature of these mutations is still a challenge. In zebrafish, as in other vertebrates, many genes have been cloned on the basis of sequence similarity to genes from other organisms. In only a few fortuitous cases has an existing mutant been found to correspond to a mutation in a cloned gene (SCHULTE-MERKER *et al.* 1994; TALBOT *et al.* 1995; SEPICH and WESTERFIELD 1993). A method to generate and identify mutations that affect a chosen gene is an important complementary strategy. We have developed a polymerase chain reaction (PCR)-based method that allows fast and efficient screening for mutations on the basis of their molecular rather than morphological defects, providing a basis for analyzing the functions of these genes.

Gamma-rays are an efficient mutagen in zebrafish (CHAKRABARTI *et al.* 1983; WALKER and STREISINGER 1983), producing a very high specific locus mutation rate of ~1:100. Gamma-ray mutagenesis has mainly been used in screens for morphological defects to identify potentially interesting mutants that affect zebrafish embryogenesis (KIMMEL 1989). Several gamma-ray induced mutations have been described in the literature (GRUNWALD *et al.* 1988; FELSENFELD *et al.* 1990; WESTERFIELD *et al.* 1990; HATTA *et al.* 1991; HALPERN *et al.* 1993; TALBOT *et al.* 1995), however, with the exception of the *ntl*^{b160} (SCHULTE-MERKER *et al.* 1994), *flh*^{b327} (TALBOT *et al.* 1995), and *nic1*^{b107} (SEPICH and WESTERFIELD 1993) mutations, very little is known about the molecular nature of these events. Ionizing radiation, such as gamma-rays, can induce a variety of chromosomal changes, that are probably best documented for X-ray induced mutations in Drosophila (CHIA *et al.* 1985; KELLEY *et al.* 1985; PASTINK *et al.* 1987, 1988; BATZER *et al.* 1988; EEKEN *et al.* 1989, 1994; MAHMOUD *et al.* 1991; LINDSLEY and ZIMM 1992). These mutations include point mutations, deletions ranging in size from a few basepairs to megabases, inversions, and translocations. Ionizing radiation induced mutations have also been extensively studied and used in mouse (VAN BUUL *et al.* 1990; CATTANACH *et al.* 1993; GOSSEN *et al.* 1995; TEASE and FISHER 1996a,b) and medaka (KUBOTA *et al.* 1992, 1995; SHIMA and SHIMADA 1994).

The spectrum of mutations induced by ionizing radiation has also been investigated in various human and hamster cell lines, primarily by Southern blot analysis of the hypoxanthine-guanine phosphoribosyltransferase (*hprt*) locus (TACHIBANA *et al.* 1990; NELSON *et al.* 1994, 1995; PUCK and HARVEY 1995). Recently, several groups have developed a multiplex PCR method to analyze these radiation induced mutations at the *hprt* locus (ROSSITER *et al.* 1991; FUSCOE *et al.* 1992; YU *et al.* 1992; ZU *et al.* 1993; NELSON *et al.* 1994; SCHWARTZ *et al.* 1994; KAGAWA *et al.* 1995; PARK *et al.* 1995). These studies

Corresponding author: Andreas Fritz, Institute of Neuroscience, 1254 University of Oregon, Eugene, OR 97403-1254.
E-mail: fritz@uoneuro.uoregon.edu

showed that >50% of gamma-ray induced alterations were large deficiencies, readily detectable by PCR screening.

We adapted the multiplex PCR method to identify mutations that affect cloned genes in zebrafish by analyzing the genomic DNA (gDNA) of parthenogenetic haploid offspring of females carrying gamma-ray induced mutations. We characterized these mutations using the genetic linkage map of the zebrafish genome (POSTLETHWAIT *et al.* 1994; JOHNSON *et al.* 1996). Our results demonstrate that gamma rays induce translocations and deletions at high frequency in the zebrafish genome, making the identification and recovery of mutations that include selected loci efficient. Some chromosomal regions show a significantly higher mutation rate than average, suggesting the existence of "hot spots" for gamma-ray induced mutations. We discuss the type of chromosomal lesions and phenotypes of three mutations isolated in the PCR screen that are representative of the range of molecular and morphological defects observed.

MATERIALS AND METHODS

Fish strains: A substrain of the Oregon AB line (WESTERFIELD 1995) was used for all mutagenesis experiments. This AB substrain was derived from gynogenetic offspring of 21 AB founder females which were free of visible embryonic mutations. The AB strain was also used in crosses with mutant fish. *T(msxB)^{b220}* mutant fish were crossed to *leopard^{tl}* (*leo*) fish, originally obtained from the NÜSSLEIN-VOLHARD lab at Tubingen and kindly provided by S. L. JOHNSON.

Staging: Embryos were developmentally staged according to standard criteria (KIMMEL *et al.* 1995), expressed as hours (hr) or days (day) post fertilization at 28.5°.

Irradiation: Sperm were collected and irradiated in a Gammatory-M irradiator with a cesium-137 source as described (WESTERFIELD 1995).

Haploid embryos: Eggs were obtained by gently squeezing the abdomens of anesthetized females. The eggs were then activated by addition of UV-treated sperm, which do not make a genetic contribution to the offspring (STREISINGER *et al.* 1981).

Genomic DNA preparation: Because haploid embryos from each female were analyzed individually, we needed to conduct a large number of genomic DNA (gDNA) extractions and PCRs with maximal reproducibility and minimal handling. Most importantly, using a strain of fish carrying a stably integrated transgene (STUART *et al.* 1988) as a target for PCR amplification, we learned that it is necessary to remove the chorion from the embryo prior to gDNA extraction to avoid contamination by wild-type sperm gDNA, presumably attached to the chorion (data not shown). For primary screening, 10 haploid embryos from each G0 female were randomly collected either at 10 or 24 hr and were manually removed from their chorions. Single embryos were placed into 0.2-ml PCR tubes (Robbins Scientific, #1044-50-0) and excess liquid removed. Either 20 μl (10 hr) or 25 μl (24 hr) of digest buffer was added to each tube. Digest buffer is 10× ThermoPol Reaction Buffer for Thermophilic DNA Polymerases (New England Biolabs, #007-TDP), diluted in sterile deionized water to 1× final concentration, and 100 μg/ml final concentration of Proteinase K. The embryos were digested for 1–3 hr at 55°, followed by 5 min at 100°, in a Programmable Thermal Controller with a Hot Bonnet lid (PTC-100–96V; MJ Research, Inc.), and the tubes were stored at −20° until use. Phenotypically sorted embryos either for recovery screening of F_1 females or RAPD mapping PCR were processed similarly, except that haploid embryos were digested in 30 μl digest buffer and diploid embryos in 50 μl.

Oligonucleotide primers: Primers (Table 1) were chosen with the help of the Primer Select Module of the Lasergene Program (DNASTAR, Inc.). Reverse Phase purified (RP-1) primers were obtained from DNA EXPRESS (Macromolecular Resources, Colorado State University). The lyophilized primers were resuspended in 1 ml of sterile, deionized water. Working stocks were prepared by diluting each primer to 10 μM and mixing the forward and reverse primers for each gene 1:1. Compatible primer pair combinations amplifying generally 8–11 different products were established by combining these working stocks as described in RESULTS. Aliquots of primer mixes were stored at −20° for convenience and accuracy.

Primer sequences: Listed in Table 1.

Multiplex PCR conditions: All reactions were carried out in a 20 μl volume in a PCR machine. First, 8 μl of gDNA were combined with 2 μl of primer pair mix in a 0.2 ml PCR tube and denatured for 5 min at 95° in the PTC machine and then cooled to 4°. Then 10 μl of master mix was added to each tube at 4°. Master mix contains per reaction: 1.2 μl 10x ThermoPol reaction buffer, 2 μl dNTP mix (2.5 mM each), 0.4 μl BSA (purified BSA 100x, New England Biolabs #007-BSA), 0.2 μl AmpliTaq enzyme (1 unit, Perkin-Elmer/Cetus), and 6.2 μl sterile deionized water. The tubes were then set on ice and the PCR program was started. The reaction tubes were returned to the heat block after it reached a temperature of ≥80°. The PCR amplification program was: 1. 94°, 30 s, initial cycle only; 2. 40 cycles of 92°, 30 s; 59°, 30 s; 75°, 2 min; 3. 75°, 10 min; 4. 4°, indefinite hold. Ten to 15 μl of PCR products were analyzed by electrophoresis on 2% ethidium bromide containing agarose gels in 0.5× TBE buffer.

To identify embryos by PCR analysis for recovery from the F_1 generation, generally only three primer pairs were used, the pair that failed to amplify in the embryos from the G0 female and two control pairs. For these reactions, the PCR program was reduced to 30 cycles and the 75° extension step shortened to 1.5 min.

RAPD PCR: Primers and their sequences defining random amplified polymorphic DNAs (RAPDs) were obtained from Operon Technologies (Alameda, CA). PCR using RAPD primers was carried out as described in JOHNSON *et al.* (1994), except that gDNA from embryos was extracted as described above, and the NEB 10× ThermoPol reaction buffer was used.

Nomenclature: General guidelines for naming zebrafish genes and mutants are published in Genetic Nomenclature Guide (Trends in Genetics) and in The Zebrafish Book (WESTERFIELD 1995). The chromosomal aberrations described here have been given a name based on the gene by which they were identified, with a prefix indicating the likely type of chromosomal aberration. The prefixes are based on Drosophila guidelines. *Df* indicates a simple deletion; *T* indicates a translocation. The *b*# is a unique allele designation, where *b* indicates the Eugene, Oregon, origin of the mutation. Gamma-ray mutagenized fish can carry multiple independent mutations. Thus, each F_1 line carrying a different mutation inherited from a single G0 fish is given a unique *b*#, which designates an independently segregating mutation originally identified in a G0 fish.

RESULTS

Multiplex PCR: We designed oligonucleotide primer pairs for multiplex PCR amplification of a number of

TABLE 1

Forward and reverse primers for multiplex PCR of selected zebrafish genes

Gene		Primers[a]	Product length (bp)
axial	f	GACATACGAGCAAGTGATGCA	454
	r	GCGAAAAAAGTCCAAATAACA	
dlx2	f	CCACCTCACCCCTCACC	229
	r	AGCGGCCGAGTCAAAATA	
dlx3	f	ATCTGGTTCCAGAACCGGAG	250
	r	GCTGTAAATGTGATCCCTGC	
elrC	f	ACGCCACATTACCTTTTCTTTCAC	110
	r	ATGCCGTCAACCGTTTTATCTGTA	
engl	f	ACCGAAAGCGACGATAAGCG	987
	r	CAATCGAATAGCGGCTTTGG	
eng2	f	GTCCCAGGTCTCGTAAACCA	325
	r	TCTCTGCCTCAGTGACTGTC	
goosecoid	f	ACGTGGGCACCTTGTCC	172
	r	ACCTTTCGTGCCAGTTGTT	
hoxb4	f	TGAGCCCGAACTATTCAGGG	430
	r	CCCTGTTTCTAATGTGCAGG	
hoxb5	f	CCTCCACTACCTCGGCGACG	720
	r	CCTTTTGCCGTCTGGTCCAG	
hoxb6	f	GGACCTTCGGTAACGCTGGT	494
	r	TAGCTTCGTTCCACATGGAC	
msxA	f	GTCCCACAATATGCCCTCTC	373
	r	CCAATAGGTGCAAAAGGCAG	
msxB	f	GCACCTTACGCAAGCACAAG	806
	r	TGGTCTTTCAAGGCACTTCC	
msxD	f	GAAAGTCCCTGTCCTCTCCG	569
	r	GACGGAGCTAAAATGTTCCG	
noggin	f	GTAAAAGCGGAACGAGACG	546
	r	GGTGTAGGACCAGAGCCAC	
tenascinC	f	CGCCAGTAACATTCAAACAG	192[b]
	r	ATGGCCTGCACTTTTACTGT	(295)
shh	f	TCGACAACTCAACGGAAGA	931
	r	TAGGTAACGGTCGGTCAAA	
ZF-114	f	CAGTTGTACGGAATAGCAGC	295
	r	TGGCACCGGAGAATCTGTTG	

f, forward; r, reverse. The size of each amplification product is indicated. Sources of sequences are as follows: *axial,* accession No. (acc#) Z22762 (STRAHLE *et al.* 1993); *dlx2,* acc# U03875, *dlx3,* acc# X65060 (AKIMENKO *et al.* (1994); *elrC,* acc# U17601 (GOOD 1995); *engl,* acc# X68445, *eng2,* acc# X68446 (EKKER *et al.* 1992); *goosecoid,* acc# L03395 (STACHEL *et al.* 1993); *hoxb4,* acc# M24085 (NJOLSTAD *et al.* 1988a); *hoxb5, hoxb6,* acc# X68248 (MOLVEN *et al.* 1993); *msxA,* acc# U16310, *msxB,* acc# U16311 (AKIMENKO *et al.* 1995), 1995; *msxD,* acc# X65062 (EKKER *et al.* 1992); *noggin,* A. FRITZ, unpublished; *tenascinC,* acc# U14940 (QIAO *et al.* 1995); *sonic hedgehog,* acc# Z35669 (*shh,* KRAUSS *et al.* 1993); *ZF-114,* acc# X60095 (MOLVEN *et al.* 1992).

[a] Primers are 5′–3′.

[b] Expected size of amplification product, actual size indicated in parentheses below.

zebrafish genes, based on published sequences or sequences made available to us prior to publication. 17 pairs of these primer sequences are shown in Table 1 (MATERIALS AND METHODS). Most primers were chosen so that their annealing temperatures were between 56° and 62°. Additionally, primer pairs for all the genes were selected to minimize possible primer dimer formation and to amplify a product of unique size for each gene within a range of 100–1000 bp. Because most primer predictions were based on cDNA sequences, we first tested primer pairs individually on zebrafish gDNA to verify that they yielded a robust amplification product of the expected size. Fourteen of 20 primer pairs amplified the expected product, one pair produced no amplification product, and five pairs amplified products larger than predicted from the cDNA sequences, presumably because introns were located between the priming sites. Two of these latter five primer pairs were subsequently used for the PCR screen, without further confirmation of the authenticity of the amplified product; in the other cases, new primer pairs were selected.

We established the initial multiplex PCR conditions by testing various combinations of three primer pairs in a single reaction. Optimal conditions were then determined by sequential addition of individual primer pairs and by adjusting relative primer pair concentra-

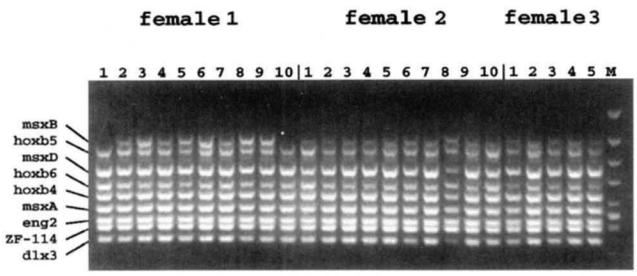

FIGURE 1.—Multiplex PCR analysis of gDNA from single haploid embryos detects gamma-ray induced mutations. Analysis of offspring from three females (female 1, female 2, female 3) is shown. The target genes are shown on the left side. Embryos 1 and 10 from female 1 lack the *msxB* specific product.

tions until all products in the mixture were amplified to approximately equal amounts. We were able to establish primer pair mixtures that reliably amplified ≤11 different products in a single reaction.

Gamma-ray mutagenesis and PCR screen: We induced gamma-ray mutations by irradiating mature sperm obtained from male AB fish. The sperm were exposed to a dose of ~250–300 rads, delivered over 35–40 sec (WESTERFIELD 1995). The irradiated sperm was then used to fertilize eggs from AB females. This dose was chosen because it was previously shown by complementation analysis to induce mutations at the *golden* locus at a high frequency (~1 in 100, see also Figure 2 in CHAKRABARTI *et al.* 1983) and because it leads to a reasonable survival of the fertilized eggs; ~25% of the embryos survive to adulthood and constitute the G0 generation. We screened the haploid offspring from the female fish of this G0 generation using the multiplex PCR assay. Haploid embryos were obtained by fertilizing the eggs of the G0 females with UV irradiated sperm, which activate development without contributing paternal genetic material (STREISINGER *et al.* 1981; WESTERFIELD 1995). We routinely assayed 10 embryos, randomly collected from each female, at either 10 or 24 hr. Figure 1 shows an example of a multiplex PCR assay using nine primer pairs per reaction. The gDNA from two of 10 embryos from one female (female 1) failed to amplify the *msxB* (HOLLAND 1991; AKIMENKO *et al.* 1995) product, suggesting that there was no *msxB* genomic template for amplification.

To recover this potential *msxB* mutation, we crossed the G0 female (female 1) to a wild-type male. We raised the F_1 generation to adulthood and analyzed the haploid offspring from F_1 females similarly to the embryos of the G0 female. We sorted the embryos from the F_1 females into morphologically distinct classes, *i.e.*, mutant and wild-type phenotypes, and analyzed embryos from each of these classes by multiplex PCR. The absence of the *msxB* PCR product correlated with one of the mutant phenotypic classes, suggesting that the loss of the PCR product was the result of a heritable mutation linked to a visible mutant phenotype. Subsequently, we isolated male F_1 fish carrying the *msxB* mutation by crossing them to their *msxB* mutant female siblings and confirmed their genotypes by PCR.

We have similarly identified 30 potential mutations by the absence of a particular PCR product after screening a total of 509 G0 females (Table 2A). Due to limitations of time and tank space, and to avoid potential PCR artifacts, we attempted to recover only 15 potential mutants for which a given PCR product was missing in at least two of the 10 embryos. We successfully reidentified all 15 of these mutations in the F_1 generation (Table 2B). Thus, considering all the potential mutants, the mutation rate was ~1 in 230 (0.0043). A more conservative estimate is 1 in 460 (0.0022), if we include only recovered mutants (Table 2A).

In parallel with the PCR screen, we examined the haploid embryos from 919 G0 females, of which the 509 of the PCR screen were a subset, for morphologically visible mutations at 24 and 48 hr (KIMMEL 1989). We scored a female as carrying a potential mutation if she produced several embryos displaying the same consistent characteristic phenotype. Phenocopies, *i.e.*, embryos with abnormal phenotypes not due to heritable mutations, usually display variable phenotypes. In this screen we found 324 (35%) females that produced offspring with phenotypes that might be due to mutations (Table 2C). This is probably an underestimate of the number of mutations present in these 919 females, because a significant fraction carried multiple mutations (see also Table 2B, *b254* and *b320*). In addition, we would have missed mutations that are either too subtle to detect morphologically or that produce phenotypes that are not visible before 3 day, after which haploid embryos die. However, conservatively, the overall frequency of morphologically detectable mutations is ~0.35 (324/919). Thus the frequency of a mutation detected by the PCR screen is ~1% of the overall mutation frequency. This estimate agrees with the previously established specific locus frequency for gamma-ray mutagenesis of ~1 in 100 (CHAKRABARTI *et al.* 1983).

The frequency of mutations generated by gamma-rays varied considerably among different chromosomal regions. The PCR screens of all 509 females included chromosomal regions, marked by two loci (*dlx 2, eng1*), in which we detected no potential mutations. In contrast, we recovered six independent alleles that delete the *hoxb4, b5,* and *b6* genes, out of a total of 398 females screened, resulting in a mutation rate of 1 in 66.3 for the chromosomal region containing these loci.

Examples of recovered mutants: The mutations we identified with the multiplex PCR screen can be broadly classified into three categories by segregation analysis: class I: reciprocal translocations in which the two partners segregate and can be propagated independently. Class II: balanced reciprocal translocations, in which both translocation partners must be present for survival.

TABLE 2

Summary of PCR screen

A. Summary of PCR screen

Total no. of females screened: 509
Average no. of loci/screen: 13.6
Total no. of potential mutants: 30
Total no. of recovered mutants: 15
Average frequency/locus:
Potential mutants: 1/230
Recovered mutants: 1/460

B. Gene(s)	Allele designation	Type and size of deficiency
dlx3	b254[a]	NA
	b320[a]	NA
	b380	Df, <8 cM
elrC	b491[b]	CR, ~80 cM
eng2	b243	T, 40–60 cM
	b320[a]	NA
gsc	b250	T, ~80 cM
hoxb4,5,6	b237[c]	T, 40–70 cM
	b245	T, 37–60 cM
	b254[a]	NA
	b308	CR, 100–160 cM
	b447	T, 37–60 cM
	b491[b]	CR, ~80 cM
msxB	b220	T[d], 15–40 cM
tenascinC	b345	Df, <10 cM
ZF-114	b316	T, 7–35 cM

C. Summary of morphology screen

Total no. of females screened: 919
Total no. of females with potential mutants: 324
Estimated mutation frequency: 1/2.8

A shows the statistical evaluation of PCR screen. In B, the left column indicates the gene(s) for which mutations were isolated in the PCR screen. The middle column shows allele designations; multiple independent alleles have been found for three different loci. The right column shows the type and size of each deficiency. CR, complex rearrangement; NA, not available; T, translocation; Df, deletion. C provides a summary of the screen of haploid offspring from G0 females for morphological defects. The 509 G0 females used in the PCR screen are a subset of the females used in the morphology screen.

[a] The 2 G0 females from which the F1 lines *b254* and *b320* were generated each carried two independent mutations (and would have been given two *b#s* each according to the nomenclature conventions), leading to a total of 15 mutations identified and recovered; however, the *b254* and *b320* lines have been terminated.

[b] *b491* deletes the *hoxb* and *elrC* genes; the *hoxb* cluster and *elrC* map to LG3. The other *hoxb* deficiencies do not affect *elrC*.

[c] The *b237* line has been terminated.

[d] The *b220* translocation has resolved (see RESULTS).

Class III: mutations that are inherited as simple deficiencies. We describe here one example of each.

Class I, the *T(msxB)*^{b220} mutation: We found the *T(msxB)*^{b220} mutation in a G0 female in which two out of 10 embryos were lacking the *msxB* (AKIMENKO *et al.* 1995) specific amplification product (see Figure 1). In the F_1 generation, seven of 15 females produced clutches of haploid embryos in which a fraction lacked the *msxB* specific amplification product and showed a distinct mutant phenotype (m1, see also Figure 4B). In the clutches of these seven females, the *msxB* deficient embryos constituted ~23% (61/274) of the total haploid offspring, while an additional 18% (49/274) of the embryos showed a second, consistent mutant phenotype (m2). The m2 phenotype includes a shortened, necrotic body axis and a distinct bulb-like tail at 24 hr (data not shown). The m2 mutant embryos die at 3 day as diploids. The remaining embryos appeared morphologically wild type, there were no apparent double mutants visible, and both the m2 and wild-type phenotypic classes amplified all 17 PCR products. We subsequently identified 4 male F_1 carriers by intercrosses. In all four crosses, the offspring consisted of morphologically wild-type embryos (654/731), the m1 (33/731) and m2 (44/731) mutant classes of embryos, and no phenotypically obvious double mutants. As in the haploid embryos, all of the diploid embryos displaying the m1 phenotype were also missing the *msxB* amplification product. Thus, the segregation ratios observed among the haploid and diploid offspring suggest that the *T(msxB)*^{b220} mutation was caused by a reciprocal translocation event. However, we have not examined the *msxB* deficient chromosome to learn whether it carries sequences from another chromosome.

In a reciprocal translocation mutation, both mutant phenotypes are visible in 1/16 embryos of a clutch, while a cross between a translocation mutation and a noncomplementing simple deletion should produce only one phenotype in 1/8 of the offspring. Consistent with this formal expectation, a subsequent cross of one of the *T(msxB)*^{b220} carrier females to a male sibling produced only wild-type (140/157, 89%) and *msxB* deficient mutant embryos (17/157, 11%); no embryos of the m2 phenotype were observed. This suggested that the male F_1 fish was heterozygous for the *msxB* deficiency, that the two translocation partners can segregate independently, and that fish inheriting only the *msxB* deficient translocation partner are viable. We confirmed in subsequent crosses, including the non-complementation cross to the *leo* pigment mutant (see below), that the reciprocal translocation partner (m2) of the *T(msxB)*^{b220} mutation is not obligate. The *T(msxB)*^{b220} designation heretofore refers to the mutation carrying the *msxB* deficient chromosome in the absence of its original translocation partner.

Because the map position of the *msxB* gene was unknown at the time, we determined the position of the *T(msxB)*^{b220} mutation on the zebrafish genetic map (POSTLETHWAIT *et al.* 1994; JOHNSON *et al.* 1996) by systematically comparing RAPD markers between gDNA from *T(msxB)*^{b220} mutant embryos and their wild-type siblings. We found three RAPD markers, *17X.640*, *2V.310*, and *20K.1450* (Figure 2, LG1) that were consis-

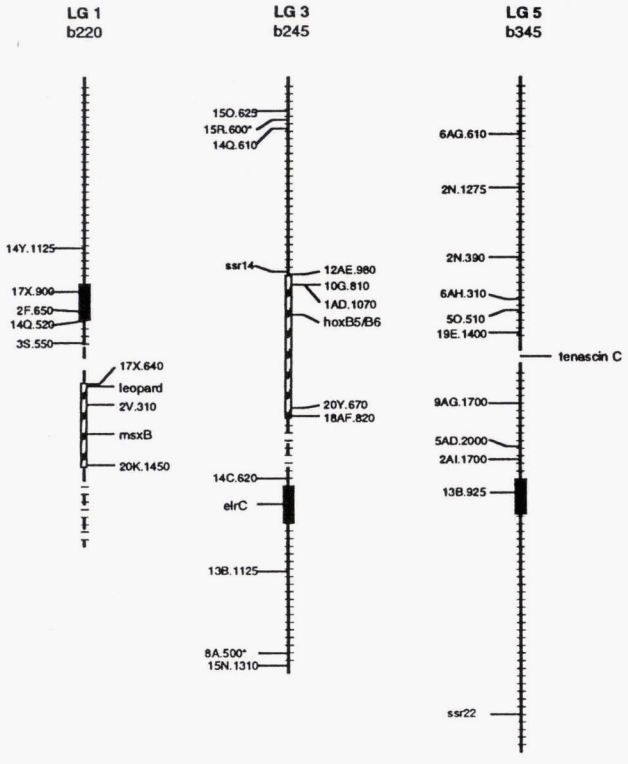

FIGURE 2.—Gamma-rays produce a range of chromosomal defects. Mapping analysis of the $T(msxB)^{b220}$ (LG1), $T(hoxb)^{b245}$ (LG3) and $Df(ten)^{b345}$ (LG5) mutations. The cross hatching indicates 2-cM intervals. Markers and genes on the right side of each LG are missing, markers shown on the left side have been tested and are present. The broken lines indicate regions of uncertainty in $T(msxB)^{b220}$ and $T(hoxb)^{b245}$. The black boxes indicate the positions of the centromeres (JOHNSON *et al.* 1996).

tently missing in gDNA extracted from haploid $T(msxB)^{b220}$ mutant embryos but present in gDNA from their haploid wild-type siblings, suggesting that the $T(msxB)^{b220}$ mutation affects the region of linkage group 1 (LG1) containing these markers. The two available markers distal to *20K.1450* (Figure 2, LG1) were uninformative, *i.e.,* the expected PCR products were not seen in gDNA from either wild-type or mutant embryos, probably due to polymorphisms within the AB strain. The *3S.550* marker and all other tested markers near the centromere or on the other chromosome arm were present in mutant gDNA, indicating that the $T(msxB)^{b220}$ mutation is a deficiency of ≥15 cM and possibly greater than 40 cM, if the entire distal end of LG1 is missing. Subsequently, we mapped the *msxB* gene, using a polymorphism within the gene between the AB and DAR strains, to LG1 between markers *2V.310* and *20K.1450* (POSTLETHWAIT *et al.* 1994), in agreement with the map position of the mutation.

The extent of the $T(msxB)^{b220}$ deficiency in LG1 predicted that the *leo* locus, which is just distal to the *17X.640* marker, should also be missing. The leo^{t1} allele causes a recessive, homozygous viable pigment mutation (Figure 3) that can be easily recognized in fish after

FIGURE 3.—The $T(msxB)^{b220}$ mutation also affects *leo*. Offspring of a $b220/+ \times leo^{t1}/leo^{t1}$ cross at 2 mon of age. (Top) $leo^{t1}/+$ genotype. (Bottom) $T(msxB)^{b220}/leo^{t1}$ genotype; the *leo* phenotype is indistinguishable from that of the leo^{t1}/leo^{t1} parent (not shown). The scale bar indicates 1 cm.

the age of 4 weeks (KIRSCHBAUM 1975). To examine whether *leo* was affected by the $T(msxB)^{b220}$ mutation, we raised to adulthood 25 offspring of a cross between a homozygous leo^{t1} male and one of the identified F_1 females carrying the original translocation mutation. Five individuals from this F_2 generation displayed a *leo* phenotype that was indistinguishable from the leo^{t1} mutant phenotype (Figure 3; JOHNSON *et al.* 1995). The outcome of this cross also confirmed our expectation that the original mutation was a translocation and that, at least, the *msxB* deficient partner of the original $T(msxB)^{b220}$ mutation can be maintained independently. If the *b220* mutation had been a simple deletion in LG1, we would have expected half of the progeny to show the *leo* phenotype; if the large deficiency in LG1 had shown haploinsufficiency and could only be maintained in the presence of its translocation partner, we would not have expected to see offspring displaying the *leo* phenotype. To confirm the predicted genotype of these fish, we analyzed embryos from intercrosses of putative $leo^{t1}/T(msxB)^{b220}$ individuals. As expected, the phenotype associated with the *msxB* deficiency constituted ~25% (42/199) of the embryos.

The $T(msxB)^{b220}$ mutant embryos, from 16 to 36 hr, suffer from cell death in the dorsal CNS at most axial levels. Figure 4B shows the phenotype of a live 32 hr $T(msxB)^{b220}$ diploid mutant embryo in comparison to a wild-type embryo of the same age (Figure 4A). Subsequently, the dying cells are cleared from the spinal cord. Eye formation is severely disturbed, as are the median and pectoral fins. The mutant embryos fail to form blood, and die at ~4 day.

Class II, the $T(hoxb)^{b245}$ mutation: We identified the $T(hoxb)^{b245}$ mutation in a G0 female, from which three out of 10 haploid offspring lacked the PCR products of the *hoxb4* (NJOLSTAD *et al.* 1988a), *hoxb5*, and *hoxb6* genes (MOLVEN *et al.* 1993). Female and male F_1 $T(hoxb)^{b245}$ carriers were recovered as described above. The frequency of *hoxb* gene deficient mutant embryos

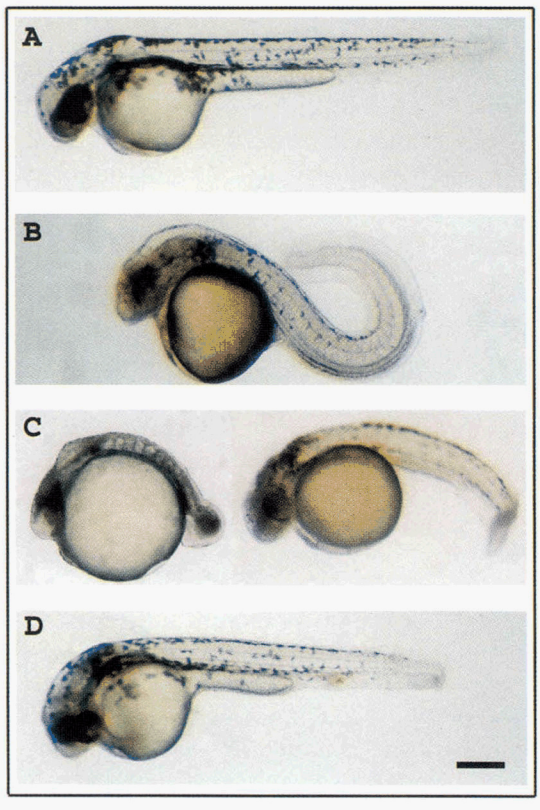

FIGURE 4.—PCR mutants have morphological defects. Live diploid embryos. Haploid phenotypes appear essentially the same. All views are lateral, anterior is to the left and dorsal is up. (A) Wild type (34 hr). (B) *T(msxB)*^{b220} mutant embryo (34 hr). (C) Left: 32 hr *T(hoxb)*^{b245} mutant embryo; right: 36 hr *T(hoxb)*^{b245} associated phenotype. (D) *Df(ten)*^{b345} mutant embryo (34 hr). See text for description of phenotypes. The scale bar in the lower right indicates 250 μm.

among haploid offspring was 24% (266/1107), and among diploid offspring the mutant phenotype constituted 3.8% (84/2194). These frequencies have been maintained through several generations of crosses to wild-type fish. Furthermore, we observed a second mutant phenotype among haploid and diploid offspring from *T(hoxb)*^{b245} parents, that consistently cosegregated with the *hoxb* deficient mutant phenotype (see below and Figure 4C). Together, these observations suggest that the *T(hoxb)*^{b245} mutation is a reciprocal translocation, in which the two translocation partners can not be maintained separately. We confirmed the translocation nature of the *T(hoxb)*^{b245} mutation directly using an allelic polymorphism within the *hoxb* cluster in the Oregon AB line; 25% of the haploid embryos from a *T(hoxb)*^{b245} carrier female inherit both allelic variants of the *hoxb* locus (data not shown), one variant from the wild-type locus on LG3 and the second variant from the translocated copy.

Mapping analysis revealed that an internal piece of LG3 is missing in gDNA from *T(hoxb)*^{b245} deficient embryos (Figure 2, LG3). Additionally, we found that the *ssr14* marker, the first marker distal to the region deleted in *T(hoxb)*^{b245} embryos, still segregates with the centromere of LG3 in gDNA from mutant embryos, suggesting that the deficiency in LG3 is a large internal deletion. Based on the currently available markers for LG3, the predicted size of the deficiency is minimally 37 cM and may be as large as 60 cM. Because of the size of this deficiency, it is likely that the entire *hoxb* cluster was translocated, although we have direct evidence from PCR for the *hoxb2, b4, b5,* and *b6* genes only.

Development in *T(hoxb)*^{b245} mutant embryos (Figure 4C) proceeds fairly normally through gastrulation and into the early segmentation period. At about the four somite stage (11.5 hr), development begins to slow and essentially arrests after formation of the 12th somite (15 hr). Cell death in the brain begins at the four somite stage, mainly in a medial stripe of cells in the hindbrain. At this stage, cells lateral to the CNS in the trunk also die and further tail development fails; cells instead accumulate in the tail bud and eventually die. The embryos die ~2 day. Figure 4C also shows a 36-hr diploid embryo displaying the second phenotype that consistently cosegregates with the *T(hoxb)*^{b245} mutant phenotype. Cell death in the midbrain and hindbrain becomes apparent ~15 hr, and there are no obvious defects in the trunk and tail. The embryos appear developmentally retarded and die ~4 day.

Class III, the *Df(ten)*^{b345} mutation: We identified a mutation deleting the zebrafish *tenascin C* (*tenC*) (QIAO *et al.* 1995; TONGIORGI *et al.* 1995) specific amplification product in six of 10 haploid embryos from a G0 female. We inspected the remaining live haploid embryos of this G0 female morphologically and found that about half of the embryos (11/21) displayed a visible mutant phenotype by 30 hr and died by 48 hr. The absence of the *tenC* product correlated with this observed mutant phenotype; gDNA from phenotypically mutant embryos failed to amplify the *tenC* PCR product. We subsequently intercrossed F_1 progeny of the founder female to analyze the segregation of the *Df(ten)*^{b345} mutation in diploid embryos. As expected from the segregation frequency of the haploid offspring in the G0 female, ~25% (84/380) of the embryos displayed the *Df(ten)*^{b345} mutant phenotype, and consistently failed to amplify the *tenC* specific PCR product.

The *Df(ten)*^{b345} mutation has affected <10 cM of the genomic region around the *tenC* gene; the nearest informative markers are all unaffected in the *Df(ten)*^{b345} mutation (Figure 2, LG5). To analyze the mutation further, we cloned ~19 kb of gDNA containing most of the *tenC* gene and 3′ flanking sequence and isolated restriction fragments from this genomic clone to generate probes for hybridization. Southern blots of gDNA from mutant embryos failed to give a hybridization signal (data not shown). Thus, this result and the segregation patterns of the mutation observed in the G0 female

and the F_1 generation show that the *Df(ten)*^{b345} mutation is a deletion.

Df(ten)^{b345} embryos appear normal at 24 hr, although many embryonic tissues express the *tenC* gene beginning at ~16 hr (TONGIORGI *et al.* 1995). Analysis of mutant embryos with a variety of RNA *in situ* and antibody probes has thus far not revealed any recognizable patterning or differentiation defects at 24 hr. Morphologically, *Df(ten)*^{b345} mutant embryos can be recognized starting at ~28 hr. In wild-type embryos at this stage, the head lifts off the yolk and straightens, and the circulatory system and blood have formed and are visible (KIMMEL *et al.* 1995). Both of these processes are impeded in mutant embryos (shown in Figure 4C at 32 hr). The head remains in close apposition to the yolk; red blood cells fail to circulate properly and aggregate in clumps, most prominently where the blood island forms. Between 40 and 50 hr, rapid deterioration and cell death throughout the embryo sets in and the mutant embryos die and disintegrate.

DISCUSSION

We have shown that a multiplex PCR method provides an efficient strategy for screening gamma-ray mutagenized fish to identify mutations affecting specific zebrafish genes. Mutations affecting genomic regions in which genes of interest are located can be detected with frequencies approaching those previously reported using complementation analysis (CHAKRABARTI *et al.* 1983; WALKER and STREISINGER 1983).

The feasibility of this mutant screen largely depends upon the ability to analyze parthenogenetically derived haploid offspring. We can detect mutations in the F_1 generation directly, and thus much greater numbers of mutagenized fish can be analyzed than would be possible in a F_2 screen. More importantly, mutations caused by deletions are represented in one half of haploid embryos, and translocation mutants are detectable with our screen in one quarter of a haploid clutch. Thus, by screening 10 haploid embryos, randomly selected before morphological phenotypes might be visible, the probability that either type of mutation will be represented in these 10 embryos is >90%. In diploid offspring, translocation mutations are present in only 1/16 of the clutch, thus requiring greater numbers of embryos, or a morphological prescreen to select for potential mutants. A prescreen would almost certainly introduce a bias for or against certain types of mutants. Our current screen can be carried out without any knowledge or assumptions about mutant phenotypes, and it allows the identification of mutations affecting genes that have no visible embryonic phenotype, or whose phenotype is masked by a mutation in a linked gene.

We observed an average locus specific mutation frequency of 0.0022 (Table 2A), which is lower than the previously published value. Complementation analysis at three independent pigment loci (*golden, brass, albino;* CHAKRABARTI *et al.* 1983) had previously shown that the locus specific mutation rate in sperm irradiated with gamma-rays is approximately 0.01 at the dose used in our experiments (see also Table 1 and Figure 2 in CHAKRABARTI *et al.* 1983). Furthermore, the ratio of recessive lethal to specific locus frequencies suggested that most deficiencies are large events, presumably deleting not only the gene analyzed, but also neighboring loci, which should be easily detectable by PCR. However, it is possible that a sizable fraction of mutations that are uncovered by complementation analysis escape detection by PCR. Analysis of the mutation spectrum induced by ionizing radiation in various mammalian cell lines suggested that ~50% of mutations exhibit large deletions affecting more than a single gene (MORRIS *et al.* 1993; SCHWARTZ *et al.* 1994; PARK *et al.* 1995), while the other mutations affected only part of a gene. Our assay should detect small intragenic deletions if they exceed ~10% of the amplified fragment length, but mutations will go undetected if they are in the gene but outside the PCR amplified target or if they are too small to detect even if they fall within the amplified region of the gene. Moreover, detection of mutations such as inversions, duplications, or insertions by PCR is only possible if the chromosomal breakpoints fall between the priming sites. Thus the frequency of mutations detected by complementation analysis could be expected to be higher than by PCR.

Other factors might contribute to the reduced average locus specific mutation rate. Thirty-fold differences have been observed between the frequencies of X-ray induced mutations at specific loci in mice (RUSSELL and RUSSELL 1959). For example there may be a correlation between gamma-ray induced mutation frequencies and spontaneous frequencies as observed in Drosophila (SHUKLA *et al.* 1979). The *golden, brass* and *albino* mutations used in zebrafish as tester loci for noncomplementation screens have arisen spontaneously, and thus the mutation rate established using these loci may be higher than for other genes. Within our more limited data set, only mutations affecting the region of LG3 containing the *hoxb* gene cluster have occurred at a frequency similar to the rate demonstrated for the pigmentation loci. If the pigmentation loci and the region on LG3 containing the *hoxb* locus represent "hot spots" for the induction of mutations, then the mutation rate for other, average loci would be lower. In addition, we did not attempt to recover 15 additional potential mutations that we had seen in only one of 10 embryos of a G0 female. At least some of these might have been bona fide mutations, and their recovery would have increased our measure of the average locus specific mutation rate.

In zebrafish, the molecular nature of gamma-ray induced alterations has been characterized only for the

ntl^{b160}, *flh*^{b327}, and *nic1*^{b107} mutations (SEPICH and WESTERFIELD 1993; SCHULTE-MERKER *et al.* 1994; TALBOT *et al.* 1995). The *ntl*^{b160} and *nic1*^{b107} mutations were both selected in morphology screens, which were strongly biased toward "clean" phenotypes and thus were more likely to represent single gene mutations. The *ntl*^{b160} mutation replaced two nucleotides in the wild-type sequence by six nucleotides within the open reading frame, leading to a frame shift and a truncated protein product. In the *nic1*^{b107} mutation, a deletion of ~1.5 kb appears to prevent the expression of an intact acetylcholine receptor alpha subunit. *flh*^{b327} is a deletion, isolated in a noncomplementation screen using *flh*^{n1} tester fish, that removes the entire *flh* gene and probably one or more closely linked genes (TALBOT *et al.* 1995). In the present screen, we recovered 15 independent gamma-ray induced mutants. Two mutations [including *Df(ten)*^{b345}] produced phenotypes in 50% of the haploid embryos of the G0 female, and the segregation patterns of these two mutations in subsequent generations confirmed that they are inherited as simple deficiencies. Both of these mutations are deletions that do not affect the nearest markers on the map. The majority of mutants we isolated (13 of 15) showed segregation patterns consistent with complex rearrangements, such as translocation events. The mapping analysis of several of these mutations, including *T(msxB)*^{b220} and *T(hoxb)*^{b245}, showed that the size of these translocations is in the order of 30 cM, or ~1% of the genome; the zebrafish genetic map spans ~2900 cM (JOHNSON *et al.* 1996). These examples demonstrate that gamma-rays produce a wide range of mutations in zebrafish, as has been shown for other genomes, and that the type of screen will bias the types of mutations obtained.

We have analyzed the segregation patterns for at least three generations of five mutations originally identified as translocations, including *T(msxB)*^{b220} and *T(hoxb)*^{b245}. The two partners of the *T(msxB)*^{b220} translocation separated in the F_1 generation, and the *msxB* deficient partner has been maintained in heterozygous form without apparent effect on viability or fertility through several generations. The four other mutations include *hox* clusters, such as *T(hoxb)*^{b245}, and can be propagated only with both translocation partners present, indicating haploinsufficiency in the regions affected by these mutations. One factor that might contribute to the haploinsufficiency syndrome of the mutations affecting the *hox* gene clusters is genetic interactions among *hox* genes. This effect, nonallelic non-complementation, has recently been demonstrated for the *HoxB5* and *HoxB6* genes in mouse (RANCOURT *et al.* 1995); mutations affecting as few as two genes within a *hox* cluster may be lethal in heterozygous form.

Prospects and conclusions: The ease with which gamma-ray induced mutations can be screened and identified by the multiplex PCR assay suggests that deficiencies including selected genes in many regions of the zebrafish genome can be isolated efficiently. Furthermore, oligonucleotide primers suitable for multiplex PCR can be obtained from the RAPD markers of the zebrafish genome map by creating sequence-tagged site markers (POSTLETHWAIT *et al.* 1994; JOHNSON *et al.* 1996), making it possible to identify deficiencies at any region of choice.

Gamma-ray induced deficiencies provide an important resource for genetic analysis. The availability of radiation induced aberrations that span nearly every segment of the Drosophila genome has played a critical role in the identification and characterization of many genes, and has provided a valuable tool for mapping and for establishing balancer chromosomes (LINDSLEY *et al.* 1972; LINDSLEY and ZIMM 1992; GARC'IA BELLIDO and WANDOSELL 1978). A standard approach to identify mutations in a newly isolated Drosophila gene is to determine its map position and use an appropriate deficiency to detect noncomplementing ethyl methanesulfonate (EMS) or *P*-element induced mutations. This approach, using the chemical ethylnitrosourea (ENU), is already being employed in mouse to obtain a complete physical and genetic description of a few regions defined by deletions (RINCHIK 1991). Efforts to obtain extensive sets of overlapping deletions that span mouse chromosomes using the chemical mutagen chlorambucil (CHL) have been initiated (RINCHIK *et al.* 1990), even though they will require large resources and facilities.

Only a minority of the mutations isolated by the multiplex PCR assay, such as potentially *Df(ten)*^{b345}, are sufficiently small that they may disrupt the function of a single gene; in most cases, these mutations will also affect neighboring loci. Although the mutant phenotype cannot be attributed to a single gene, by analyzing aspects of the phenotype using molecular markers, a "candidate" phenotype can be determined that correlates with the expression pattern of the known gene. This information can be used to discriminate among the increasing number of existing chemically induced mutations for those that might affect a single gene within the deficiency. More importantly, the function of individual genes within large deficiencies can be studied by isolating new alleles in noncomplementation screens. RILEY and GRUNWALD (1995) have developed a mutagenesis protocol using ENU, which induces point mutations at very high specific locus frequencies in zebrafish. Thus, by crossing ENU-mutagenized fish to fish carrying the deficiency mutations reported here, it will be feasible to conduct efficient saturation mutagenesis of a small chromosomal region for point mutations by noncomplementation screens. The PCR selected deficiencies provide a null phenotype background, thus simplifying the identification of ENU-induced mutations, including hypomorphic alleles that might otherwise be difficult to recognize.

We are grateful to STEPHEN DEVOTO, STEPHEN JOHNSON, CHARLES KIMMEL and JOHN POSTLETHWAIT for their comments on the manuscript. We thank MICHAEL GATES and SCOTT STAWICKI for their help with mapping genes. This work was supported in part by an EMBO and a Swiss National Foundation Grant to A.F. and by National Institutes of Health grant HD-22486.

LITERATURE CITED

AKIMENKO, M. A., M. EKKER, J. WEGNER, W. LIN and M. WESTERFIELD, 1994 Combinatorial expression of three zebrafish genes related to distal-less: part of a homeobox gene code for the head. J. Neurosci. **14:** 3475–3486.

AKIMENKO, M. A., S. L. JOHNSON, M. WESTERFIELD and M. EKKER, 1995 Differential induction of four msx homeobox genes during fin development and regeneration in zebrafish. Development **121:** 347–357.

BATZER, M. A., B. TEDESCHI, N. G. FOSSETT, A. TUCKER, G. KILROY *et al.*, 1988 Spectra of molecular changes induced in DNA of Drosophila spermatozoa by 1-ethyl-1-nitrosourea and X-rays. Mutat. Res. **199:** 255–268.

CATTANACH, B. M., M. D. BURTENSHAW, C. RASBERRY and E. P. EVANS, 1993 Large deletions and other gross forms of chromosome imbalance compatible with viability and fertility in the mouse. Nat. Genet. **3:** 56–61.

CHAKRABARTI, S., G. STREISINGER, F. SINGER and C. WALKER, 1983 Frequency of gamma-ray induced specific locus and recessive lethal mutations in mature germ cells of the zebrafish, *Brachydanio Rerio.* Genetics **103:** 109–123.

CHIA, W., C. SAVAKIS, R. KARP, H. PELHAM and M. ASHBURNER, 1985 Mutation of the Adh gene of Drosophila melanogaster containing an internal tandem duplication. J. Mol. Biol. **186:** 679–688.

DRIEVER, W., D. STEMPLE, A. SCHIER and L. SOLNICA-KREZEL, 1994 Zebrafish: genetic tools for studying vertebrate development. Trends Genet. **10:** 152–159.

EEKEN, J. C., A. W. DE JONG, M. LOOS, C. VREEKEN, R. ROMEYN *et al.*, 1994 The nature of X-ray-induced mutations in mature sperm and spermatogonial cells of Drosophila melanogaster. Mutat. Res. **307:** 201–212.

EEKEN, J. C., A. PASTINK, M. NIVARD, E. W. VOGEL and F. H. SOBELS, 1989 The nature of X-ray and chemically induced mutations in Drosophila in relation with DNA repair. Ann. Ist. Super. Sanita **25:** 213–218.

EKKER, M., J. WEGNER, M. A. AKIMENKO and M. WESTERFIELD, 1992 Coordinate embryonic expression of three zebrafish engrailed genes. Development **116:** 1001–1010.

FELSENFELD, A. L., C. WALKER, M. WESTERFIELD, C. KIMMEL and G. STREISINGER, 1990 Mutations affecting skeletal muscle myofibril structure in the zebrafish. Development **108:** 443–459.

FUSCOE, J. C., L. J. ZIMMERMAN, A. FEKETE, R. W. SETZER and B. J. ROSSITER, 1992 Analysis of X-ray-induced HPRT mutations in CHO cells: insertion and deletions. Mutat. Res. **269:** 171–183.

GARC'IA BELLIDO, A., and F. WANDOSELL, 1978 The effect of inversions on mitotic recombination in *Drosophila melanogaster.* Mol. Gen. Genet. **161:** 317–321.

GOOD, P. J., 1995 A conserved family of elav-like genes in vertebrates. Proc. Natl. Acad. Sci. USA **92:** 4557–4561.

GOSSEN, J. A., H. J. MARTUS, J. Y. WEI and J. VIJG, 1995 Spontaneous and X-ray-induced deletion mutations in a LacZ plasmid-based transgenic mouse model. Mutat. Res. **331:** 89–97.

GRUNWALD, D. J., C. B. KIMMEL, M. WESTERFIELD, C. WALKER and G. STREISINGER, 1988 A neural degeneration mutation that spares primary neurons in the zebrafish. Dev. Biol. **126:** 115–128.

HALPERN, M. E., R. K. HO, C. WALKER and C. B. KIMMEL, 1993 Induction of muscle pioneers and floor plate is distinguished by the zebrafish no tail mutation. Cell **75:** 99–111.

HATTA, K., C. B. KIMMEL, R. K. HO and C. WALKER, 1991 The cyclops mutation blocks specification of the floor plate of the zebrafish central nervous system. Nature **350:** 339–341.

HOLLAND, P. W., 1991 Cloning and evolutionary analysis of msh-like homeobox genes from mouse, zebrafish and ascidian. Gene **98:** 253–257.

JOHNSON, S. L., D. AFRICA, C. WALKER and J. A. WESTON, 1995 Genetic control of adult pigment stripe development in zebrafish. Dev. Biol. **167:** 27–33.

JOHNSON, S. L., M. A. GATES, M. JOHNSON, W. S. TALBOT, S. HORNE *et al.*, 1996 Centromere-linkage analysis and consolidation of the zebrafish genetic map. Genetics **142:** 1277–1288.

JOHNSON, S. L., C. N. MIDSON, E. W. BALLINGER and J. H. POSTLETHWAIT, 1994 Identification of RAPD primers that reveal extensive polymorphisms between laboratory strains of zebrafish. Genomics **19:** 152–156.

KAGAWA, Y., F. YATAGAI, M. SUZUKI, Y. KASE, A. KOBAYASHI *et al.*, 1995 Analysis of mutations in the human HPRT gene induced by accelerated heavy-ion irradiation. J. Radiat. Res. **36:** 185–195.

KELLEY, M. R., I. P. MIMS, C. M. FARNET, S. A. DICHARRY and W. R. LEE, 1985 Molecular analysis of X-ray-induced alcohol dehydrogenase (ADH) null mutations in Drosophila melanogaster. Genetics **109:** 365–377.

KIMMEL, C. B., 1989 Genetics and early development of zebrafish. Trends Genet. **5:** 283–288.

KIMMEL, C. B., W. W. BALLARD, S. R. KIMMEL, B. ULLMANN and T. F. SCHILLING, 1995 Stages of embryonic development of the zebrafish. Dev. Dyn. **203:** 253–310.

KIRSCHBAUM, F., 1975 Untersuchungen uber das Farbmuster der Zebrabarbe *Brachydanio rerio* (Cyprinidae, Teleostei). Roux's Arch. Dev. Biol. **177:** 129–152

KRAUSS, S., J. P. CONCORDET and P. W. INGHAM, 1993 A functionally conserved homolog of the Drosophila segment polarity gene hh is expressed in tissues with polarizing activity in zebrafish embryos. Cell **75:** 1431–1444.

KUBOTA, Y., A. SHIMADA and A. SHIMA, 1992 Detection of gamma-ray-induced DNA damages in malformed dominant lethal embryos of the Japanese medaka (*Oryzias latipes*) using AP-PCR fingerprinting. Mutat. Res. **283:** 263–270.

KUBOTA, Y., A. SHIMADA and A. SHIMA, 1995 DNA alterations detected in the progeny of paternally irradiated Japanese medaka fish (*Oryzias latipes*). Proc. Natl. Acad. Sci. USA **92:** 330–334.

LINDSLEY, D. L., L. SANDLER, B. S. BAKER, A. T. CARPENTER, R. E. DENELL *et al.*, 1972 Segmental aneuploidy and the genetic gross structure of the *Drosophila* genome. Genetics **71:** 157–184.

LINDSLEY, D. L., and G. G. ZIMM, 1992 *The Genome of Drosophila melanogaster.* Academic Press, Inc., San Diego.

MAHMOUD, J., N. G. FOSSETT, P. ARBOUR REILY, M. MCDANIEL, A. TUCKER *et al.*, 1991 DNA sequence analysis of X-ray induced Adh null mutations in Drosophila melanogaster. Environ. Mol. Mutagen. **18:** 157–160.

MOLVEN, A., I. HORDVIK and P. R. NJOLSTAD, 1993 Sequence analysis of the zebrafish hox-B5/B6 region. Biochim. Biophys. Acta **1173:** 102–106.

MOLVEN, A., I. HORDVIK, P. R. NJOLSTAD, M. VAN GHELUE and A. FJOSE, 1992 The zebrafish homeobox gene hox[zf-114]: primary structure, expression pattern and evolutionary aspects. Int. J. Dev. Biol. **36:** 229–237.

MORRIS, T., W. MASSON, B. SINGLETON and J. THACKER, 1993 Analysis of large deletions in the HPRT gene of primary human fibroblasts using the polymerase chain reaction. Somat. Cell Mol. Genet. **19:** 9–19.

MULLINS, M. C., M. HAMMERSCHMIDT, P. HAFFTER and C. NÜSSLEIN-VOLHARD, 1994 Large-scale mutagenesis in the zebrafish: in search of genes controlling development in a vertebrate. Curr. Biol. **4:** 189–202.

MULLINS, M. C., and C. NÜSSLEIN-VOLHARD, 1993 Mutational approaches to studying embryonic pattern formation in the zebrafish. Curr. Opin. Genet. Dev. **3:** 648–654.

NELSON, S. L., C. R. GIVER and A. J. GROSOVSKY, 1994 Spectrum of X-ray-induced mutations in the human hprt gene. Carcinogenesis **15:** 495–502.

NELSON, S. L., I. M. JONES, J. C. FUSCOE, K. BURKHART-SCHULTZ and A. J. GROSOVSKY, 1995 Mapping the end points of large deletions affecting the hprt locus in human peripheral blood cells and cell lines. Radiat. Res. **141:** 2–10.

NJOLSTAD, P. R., A. MOLVEN, J. APOLD and A. FJOSE, 1990 The zebrafish homeobox gene hox-2.2: transcription unit, potential regulatory regions and *in situ* localization of transcripts. EMBO J. **9:** 515–524.

NJOLSTAD, P. R., A. MOLVEN and A. FJOSE, 1988a A zebrafish homologue of the murine Hox-2.1 gene. FEBS Lett. **230:** 25–30.

NJOLSTAD, P. R., A. MOLVEN, I. HORDVIK, J. APOLD and A. FJOSE, 1988b Primary structure, developmentally regulated expression and potential duplication of the zebrafish homeobox gene ZF-21. Nucleic Acids Res. **16:** 9097–9111.

NÜSSLEIN-VOLHARD, C., 1994 Of flies and fishes. Science **266:** 572–574.

PARK, M. S., T. HANKS, A. JABERABOANSARI and D. J. CHEN, 1995 Molecular analysis of gamma-ray-induced mutations at the hprt locus in primary human skin fibroblasts by multiplex polymerase chain reaction. Radiat. Res. **141:** 11–18.

PASTINK, A., A. P. SCHALET, C. VREEKEN, E. PAR'ADI and J. C. EEKEN, 1987 The nature of radiation-induced mutations at the white locus of *Drosophila melanogaster*. Mutat. Res. **177:** 101–115.

PASTINK, A., C. VREEKEN, A. P. SCHALET and J. C. EEKEN, 1988 DNA sequence analysis of X-ray-induced deletions at2 the white locus of *Drosophila melanogaster*. Mutat. Res. **207:** 23–8.

POSTLETHWAIT, J. H., S. L. JOHNSON, C. N. MIDSON, W. S. TALBOT, M. GATES *et al.*, 1994 A genetic linkage map for the zebrafish. Science **264:** 699–703.

PUCK, T. T., and W. F. HARVEY, 1995 Gamma-ray mutagenesis measurement in mammalian cells. Mutat. Res. **329:** 173–181.

QIAO, T., B. K. MADDOX and H. P. ERICKSON, 1995 A novel alternative splice domain in zebrafish tenascin-C. Gene **156:** 307–308.

RANCOURT, D. E., T. TSUZUKI and M. R. CAPECCHI, 1995 Genetic interaction between hoxb-5 and hoxb-6 is revealed by nonallelic noncomplementation. Genes Dev. **9:** 108–122.

RILEY, B. B., and D. J. GRUNWALD, 1995 Efficient induction of point mutations allowing recovery of specific locus mutations in zebrafish. Proc. Natl. Acad. Sci. USA **92:** 5997–6001.

RINCHIK, E. M., 1991 Chemical mutagenesis and fine-structure functional analysis of the mouse genome. Trends Genet. **7:** 15–21.

RINCHIK, E. M., J. W. BANGHAM, P. R. HUNSICKER, N. L. CACHEIRO, B. S. KWON *et al.*, 1990 Genetic and molecular analysis of chlorambucil-induced germ-line mutations in the mouse. Proc. Natl. Acad. Sci. USA **87:** 1416–1420.

ROSSITER, B. J., J. C. FUSCOE, D. M. MUZNY, M. FOX and C. T. CASKEY, 1991 The Chinese hamster HPRT gene: restriction map, sequence analysis, and multiplex PCR deletion screen. Genomics **9:** 247–256.

RUSSELL, W. L., and L. B. RUSSELL, 1959 The genetic and phenotypic characteristics of radiation-induced mutations in mice. Radiat. Res. (Suppl. 1) 296–305.

SCHULTE-MERKER, S., F. J. VAN EEDEN, M. E. HALPERN, C. B. KIMMEL and C. NÜSSLEIN-VOLHARD, 1994 no tail (ntl) is the zebrafish homologue of the mouse T (Brachyury) gene. Development **120:** 1009–1015.

SCHWARTZ, J. L., J. ROTMENSCH, J. SUN, J. AN, Z. XU *et al.*, 1994 Multiplex polymerase chain reaction-based deletion analysis of spontaneous, gamma ray- and alpha-induced hprt mutants of CHO-K1 cells. Mutagenesis **9:** 537–40.

SEPICH, D., and M. WESTERFIELD, 1993 Molecular characterization of a zebrafish acetylcholine receptor mutation, *nic1*. Soc. Neurosci. Abstr. **19:** 1294.

SHIMA, A., and A. SHIMADA, 1994 The Japanese medaka, Oryzias latipes, as a new model organism for studying environmental germ-cell mutagenesis. Environ. Health Perspect. **12:** 33–35.

SHUKLA, P. T., K. SANKARANARAYANAN and F. H. SOBELS, 1979 Is there a proportionality between the spontaneous and the X-ray-induction rates of mutations? Experiments with mutations at 13 X-chromosome loci in Drosophila melanogaster. Mutat. Res. **61:** 229–248.

SOLNICA-KREZEL, L., A. F. SCHIER and W. DRIEVER, 1994 Efficient recovery of ENU-induced mutations from the zebrafish germline. Genetics **136:** 1401–1420.

STACHEL, S. E., D. J. GRUNWALD and P. Z. MYERS, 1993 Lithium perturbation and goosecoid expression identify a dorsal specification pathway in the pregastrula zebrafish. Development **117:** 1261–1274.

STRAHLE, U., P. BLADER, D. HENRIQUE and P. W. INGHAM, 1993 Axial, a zebrafish gene expressed along the developing body axis, shows altered expression in cyclops mutant embryos. Genes Dev **7:** 1436–1446.

STREISINGER, G., WALKER, C., DOWER, N., KNAUBER, D. and F. SINGER, 1981 Production of clones of homozygous diploid zebra fish (*Brachydanio rerio*). Nature **291:** 293–296.

STUART, G. W., J. V. MCMURRAY and M. WESTERFIELD, 1988 Replication, integration and stable germ-line transmission of foreign sequences injected into early zebrafish embryos. Development **103:** 403–412.

TACHIBANA, A., T. OHBAYASHI, H. TAKEBE and K. TATSUMI, 1990 Molecular changes in UV-induced and gamma-ray-induced mutations in human lymphoblastoid cells. Mutat. Res. **230:** 159–166.

TALBOT, W. S., B. TREVARROW, M. E. HALPERN, A. E. MELBY, G. FARR *et al.*, 1995 A homeobox gene essential for zebrafish notochord development. Nature **378:** 150–157.

TEASE, C., and G. FISHER, 1996a Cytogenetic and genetic studies of radiation-induced chromosome damage in mouse oocytes. I. Numerical and structural chromosome anomalies in metaphase II oocytes, pre- and post-implantation embryos. Mutat. Res. **349:** 145–153.

TEASE, C., and G. FISHER, 1996b Cytogenetic and genetic studies of radiation-induced chromosome damage in mouse oocytes. II. Induced chromosome loss and dominant visible mutations. Mutat. Res. **349:** 155–162.

TONGIORGI, E., R. R. BERNHARDT, K. ZINN and M. SCHACHNER, 1995 Tenascin-C mRNA is expressed in cranial neural crest cells, in some placodal derivatives, and in discrete domains of the embryonic zebrafish brain. J Neurobiol **28:** 391–407.

VAN BUUL, P. P., A. L'EONARD and J. H. GOUDZWAARD, 1990 Dose-effect relationship for X-ray-induced reciprocal translocations in mouse spermatogonia following pretreatment with 3-aminobenzamide. Mutat. Res. **232:** 273–280.

WALKER, C., and G. STREISINGER, 1983 Induction of mutations by gamma-rays in pregonial germ cells of zebrafish embryos. Genetics **103:** 125–136.

WESTERFIELD, M., 1995 *The Zebrafish Book.* University of Oregon Press, Eugene.

WESTERFIELD, M., D. W. LIU, C. B. KIMMEL and C. WALKER, 1990 Pathfinding and synapse formation in a zebrafish mutant lacking functional acetylcholine receptors. Neuron **4:** 867–874.

YU, Y. J., Z. XU, R. A. GIBBS and A. W. HSIE, 1992 Polymerase chain reaction-based comprehensive procedure for the analysis of the mutation spectrum at the hypoxanthine-guanine phosphoribosyltransferase locus in Chinese hamster cells. Environ. Mol. Mutagen. **19:** 267–273.

ZU, Z., Y. YU, R. A. GIBBS, C. T. CASKEY and A. W. HSIE, 1993 Multiplex DNA amplification and solid-phase direct sequencing for mutation analysis at the hprt locus in Chinese hamster cells. Mutat. Res. **288:** 237–248.

Communicating editor: N. A. JENKINS